ORIGINAL ARTICLE

Enhanced Oral Delivery of Asenapine Maleate from Solid Lipid Nanoparticles: Pharmacokinetic and Brain Distribution Evaluations

Vaishali M. Gambhire, Nisharani S. Ranpise

Department of Pharmaceutics, Sinhgad College of Pharmacy, Pune, Maharashtra, India

Abstract

Introduction: The aim of the present research work was to develop asenapine maleate (AM)-loaded solid lipid nanoparticles (AM-SLN) for the enhancement of oral bioavailability of drug and delivery to the brain. **Materials and Methods:** A 3^2 factorial design was used for the development and optimization of AM-SLN. Two independent variables, drug:lipid ratio (X_1) and number of homogenization cycles (X_2), were selected, while particle size and entrapment efficiency were selected as response variables. The optimized batch was evaluated by various *in vitro* characterizations and *in vivo* pharmacokinetic and brain distribution studies. **Results:** The particle size, polydispersity index, entrapment efficiency, and zeta potential of optimized AM-SLN were found to be 113 ± 4 nm, 0.34 ± 0.05, 72.4 ± 1.73%, and −41.4 ± 2.25 mV, respectively. Pharmacokinetic study indicated significantly higher ($P < 0.05$) peak drug concentration (142.41 ± 8.14 ng/mL), area under the drug concentration-time curve (1561.81 ± 36.34 h ng/mL), and mean residence time (15.31 ± 3.21 h) of AM-SLN compared to AM-suspension (77.02 ± 5.74 ng/mL, 299.76 ± 39.42 ng/mL, and 2.73 ± 0.16 h, respectively) through oral route. Brain distribution study showed higher drug permeation across the blood–brain barriers and accumulation in the brain. **Conclusion:** These findings demonstrate that SLNs could be a new promising drug delivery system for oral delivery of AM in the treatment of schizophrenia.

Key words: Asenapine maleate, bioavailability, brain distribution, hepatic first pass, lymphatic uptake, solid lipid nanoparticles

INTRODUCTION

Schizophrenia is a serious mental disorder which is characterized by false belief, false perception, hearing voices, and seeing things which do not exist, whereas bipolar disorder is a manic-depressive illness involving alternating periods of mania and depression.[1] Schizophrenia and bipolar disorder are serious neuropsychiatric disorders with substantial health risks for patients that result in major socioeconomic burdens on the society.[2] Asenapine maleate (AM) is a novel drug (dibenzo-oxepinopyrrole), used in the acute treatment of schizophrenia and manic or mixed episodes associated with bipolar I disorder. The antipsychotic activity of AM is thought to be due to antagonistic activity on D_2 dopamine and 5-HT_2A serotonin receptors.[3] It is slightly soluble in water with free base logP 6.33 and classified as BCS class II drug. The bioavailability of AM was found to be around 35% by sublingual route, while it was <2% through oral due to its high gastrohepatic metabolism.[4]

To overcome the drawback associated with extensive metabolism and, hence, to increase the bioavailability of AM, few approaches were adopted by some of the researchers which include sublingual film,[5] intranasal,[6] and injectable[7] formulations of AM.

Although AM has therapeutic potential in the treatment of schizophrenia, its current dosage form (sublingual tablets) has

Address for correspondence:
Vaishali M. Gambhire, Department of Pharmaceutics,
Sinhgad College of Pharmacy, Vadgaon (Bk.),
Pune -411 041, Maharashtra, India.
Phone: +91-9423084869.
E-mail: vaishaligambhire@gmail.com

Received: 23-08-2017
Revised: 29-08-2018
Accepted: 08-09-2018

drawbacks such as low bioavailability, drinking and eating restriction, twice a day dosing regimen, and extrapyramidal side effect. Thus, new formulation strategies have to be adopted to overcome the problem of asenapine delivery.[8]

Even though the oral route is the most common and preferred route for drug delivery, pH of gastrointestinal tract, residence time, solubility, and hepatic first-pass metabolism can limit drug absorption or availability by this route. To avoid first-pass metabolism and improve bioavailability by the oral route, lymphatic delivery can be used as an alternative choice. Since intestinal lymph vessels drain directly into thoracic duct, further into the venous blood, thus bypassing the portal circulation, enhanced lymphatic transport of drugs reduces the hepatic first-pass metabolism.[9,10] The lymphatic system facilitates absorption of long-chain fatty acids through chylomicron formation. To enhance the lymphatic transport of drugs, two lipid-based approaches can be used such as synthesis of a highly lipophilic prodrug and incorporation of drug in a lipid carrier.[11]

It has been reported that uptake of drug occurs through the lymphatic system when encapsulated into solid lipid nanoparticles (SLNs), thus resulting into increase in oral bioavailability.[12-14] SLNs, generally spherical in shape, are a solid lipid core stabilized by a surfactant interfacial region. SLNs combine the advantages of lipid emulsion systems and polymeric nanoparticle systems while overcome the temporal and *in vivo* stability issues associated with other drug delivery approaches.[15-17] SLNs are biocompatible and biodegradable and also avoid the use of organic solvents. SLNs, due to the solid nature of the lipid matrix, can be lyophilized and transformed into the conventional oral solid dosage forms such as tablets and capsules, thus enhancing stability and patient compliance.

The nanoparticulate drug delivery, through different transport mechanisms, has exhibited great potential in brain delivery of drugs. The inherent properties of nanocarriers such as size, tailored surface, solubility improvement, release modification, and multifunctionality facilitate bioavailability enhancement and movement of drugs across blood–brain barriers (BBB). It has been reported that the lipid nanoparticles in size <200 nm are widely preferred carriers for brain delivery.[18-20]

The aim of this study was to develop AM-loaded SLN using the 3^2 factorial design. Further, *in vivo* brain and plasma pharmacokinetic studies were performed in male Wistar rats.

MATERIALS AND METHODS

Materials

AM was kindly provided by MSN Laboratories Pvt. Ltd., Telangana, India, as a gift sample. Compritol 888 ATO was procured as a gift sample from Gattefosse, India. Tween 80 and Span 80 were purchased from Loba Chemie Pvt., Ltd., Mumbai, India. Other chemicals and solvents purchased were of analytical grade and were used as received.

Preparation of SLNs

SLNs were prepared by high-pressure homogenization method.[21,22] Briefly, lipid phase consisted of AM, and lipid and lipid phase surfactant maintained at 70°C. An aqueous phase was prepared by dissolving aqueous surfactant in distilled water (sufficient to produce 100 ml of preparation) and heated to the same temperature as of lipid phase. Hot aqueous phase was added to lipid phase, and homogenization was carried out at 70°C using mechanical stirrer (Speed controller, Bio Lab, Mumbai, India) at 4000 rpm for 10 min. Coarse hot "oil in water emulsion" so obtained was subjected to further size reduction using high-pressure homogenizer (LM 10 Microfluidizer, Microfluidics, USA) at 15,000 PSI for 10–30 homogenization cycles.

Experimental design and statistical analysis

Most formulation studies involve a variation of one factor at a time, keeping other factors constant. Factorial design enables all factors to be varied simultaneously, allowing quantification of the effects caused by independent variables and interactions between them. In this study, a 3^2 full factorial experimental design was introduced to optimize the formulation of nanoparticles. Initial studies were undertaken to decide on the excipients and their levels in the experimental design.

The choice of lipid was made on the basis of solubility and partition behavior of AM in the lipid. Aqueous phase surfactant and lipid phase surfactant were selected on the basis of the stability of dispersion prepared using different surfactants. To optimize the preparation of formulations, the drug:lipid ratio (X_1) and a number of homogenization cycles (X_2) were chosen as independent variables. These two factors that might affect the nanoparticles formulation and three levels of each factor were selected [Table 1] and arranged according to a 3^2 full factorial experimental design.

Particle size and zeta potential measurement

The mean particle size and polydispersity index of the SLNs were determined by dynamic light scattering technique (which analyzes the fluctuations in light scattering due to Brownian motion of the particles) using SZ-100 HORIBA Ltd., Japan, at 25°C. The scattered light from the particles present in the sample was collected either at 90° or 173°, which was automatically selected by the instrument as the optimum scattering angle based on sample concentration. The polydispersity index was studied to determine the narrowness of the particle size distribution.

The charge on the surface of drug-loaded dispersion was determined using a zeta potential analyzer (SZ 100, HORIBA

Table 1: Independent variables and their selected levels for SLN formulation

Independent Variable	Coded levels		
	−1	0	+1
Drug: lipid ratio	1:3	1:5	1:7
Number of homogenization cycles	5	10	15

SLN: Solid lipid nanoparticles

Ltd., Japan). Laser Doppler microelectrophoresis was used to measure zeta potential. In this method, sample volumes as small as 100 µl were filled in microelectrophoresis cells to predict and control dispersion stability. An electric field was applied to a dispersion of particles. Particles within the dispersion with a zeta potential will migrate toward the electrode of opposite charge with a velocity proportional to the magnitude of the zeta potential. Analysis time was kept for 80 s, and average zeta potential, charge, and mobility of SLN batches were determined. The electrophoretic mobility was converted to zeta potential by inbuilt software using the Helmholtz–Smoluchowski equation.

Entrapment efficiency

The entrapment efficiency of prepared SLNs was calculated by the centrifugation method. About 2 ml of a dispersion of SLN and 5 ml of methanol were taken in a centrifuge tube, and further, it was centrifuged in a cooling centrifuge (REMI-C24 BL, Remi Elektrotechnik Ltd., India) at 13,000 rpm for 1 h. After centrifugation, the supernatant was removed and diluted with an appropriate solvent. The concentration of drug (free drug) in the supernatant layer was determined using UV-VIS Spectrophotometer (1800 UV/VIS, Shimadzu, Japan).

The entrapment efficiency (EE) is calculated using the following formula:

$$EE=\frac{\text{Weigh to finitial drug-weight of free drug}}{\text{Weight of initial drug}}\times 100 \quad (1)$$

Field emission scanning electron microscopy (FE-SEM)

The surface morphology of optimized SLN formulation was studied using FE-SEM (BRUKER, x-Flash 6130, USA) at 25 ± 2°C. The SLN dispersion was placed on aluminum foil and air dried for 24 h. Further, it was analyzed at ×50.000 magnification with accelerating voltage of 10 kV.

Differential scanning calorimetry (DSC)

DSC was performed by PerkinElmer 4000 (PerkinElmer, USA) instrument, and an empty standard aluminum pan was used as reference. DSC scans were recorded at the heating rate of 10°C/min in temperature range 30–350°C and 40 ml/min of nitrogen flow. DSC measurements were carried out on pure AM as bulk drug and optimized batch of AM-loaded SLNs.

X-ray diffraction

X-ray scattering measurements were carried out on a powder X-ray diffractometer (Bruker, D8 Advance, Germany) with copper as an anode material and dermic X-ray tube as a source operated at a voltage of 30 kV and a current of 30 mA. The samples were analyzed using a LynxEye detector and filtered using a Ni filter with a 2θ angle of 5–60°.

Fourier-transmission infrared spectroscopy (FTIR) studies

A FTIR spectrophotometer (Perkin Elmer, Spectrum BX, USA) was used for infrared analysis of samples. About 1–2 mg of sample was mixed with dry potassium bromide, and the samples were examined at transmission mode over a wave number range of 4000–400 cm^{-1}. FTIR studies were carried out on pure Compritol888 ATO, AM as bulk material, and SLN loaded with AM.

In vitro release of AM from SLNs

The *in vitro* release of AM from AM-SLN and AM suspension in phosphate buffer pH 7.4 and 0.1 N HCl was determined using the Dialysis Bag Diffusion Technique. In brief, SLN dispersion (containing the drug equivalent to 10 mg) was added to the dialysis bag having pore size of 2.4 nm (molecular weight cutoff 12000D) and sealed. The sealed bag was then suspended in a beaker containing 250 ml of release medium and stirred at a constant speed of 50 rpm at 37°C ± 0.5°C. Further, 10 mL of dissolution medium was withdrawn at the different time points for 12 h (0.5, 1, 2, 3, 4, 6, 8, and 12 h) and equal volume of fresh release medium was replenished. The samples were analyzed by UV-VIS spectrophotometer. Each experiment was performed in triplicate.

Pharmacokinetic studies

Animals and dosing

For *in vivo* pharmacokinetic studies, male Wistar rats weighing 250–300 g were used. All protocols involving experimental animal were approved by the Institutional Animal Ethics Committee of Sinhgad College of Pharmacy, Pune, India. The rats were randomly divided into two groups with $n = 6$ in each group to minimize the variation between individuals. One group of animals received 30 mg/kg free AM diluted in distilled water orally. The second group received 30 mg/kg AM-SLNs dispersed in distilled water just before oral administration. After administration, 20 µl of blood serial samples were withdrawn from retro-orbital route at 0.5, 1, 2, 4, 8, and 12 h. Blood samples were collected in

0.5 mL of heparinized polythene tubes and centrifuged for 10 min at 4,000 rpm and 4°C to obtain the plasma. Analyte was extracted from rat plasma by protein precipitation using acetonitrile. Acetonitrile (0.5 ml) was added in each sample and vortexed for 1 min. All samples were then centrifuged for 10 min at 3000 rpm. This procedure of protein precipitation with acetonitrile was further repeated twice with the supernatants collected. The supernatant was separated, evaporated, reconstituted with methanol, and analyzed on high-performance liquid chromatography (LC) (LC-2010C_{HT}, Shimadzu, Japan).

Data analysis

The plasma concentration-time data were analyzed and the pharmacokinetic parameters, including maximum plasma concentration (C_{max}), corresponding time (T_{max}), area under the plasma concentration-time curve (AUC), elimination half-life ($t_{1/2}$), and mean residence time (MRT), were estimated using PKsolver software.

In vivo brain distribution

After oral administration of 30 mg/kg AM suspension and AM-SLN to two groups (n = 6), animals were sacrificed and decapitated at 8 and 12 h. The brain tissue was isolated, subsequently mixed, and homogenized with 2 mL methanol for 5 min. After homogenization, brain homogenates were centrifuged; supernatants were collected. The subsequent sample preparation for brain extraction was the same as that described for the plasma extraction method.

Statistical Analysis

All data are presented as mean ± S.D. Statistical significance was evaluated using two-way ANOVA followed by Bonferroni post-test, with analysis performed using Prism 4.0 software (Graph Pad software); $P = 0.05$ and below were considered statistically significant.

RESULTS AND DISCUSSION

Diverse physiological actions are altered when drugs are delivered by intestinal lymphatic route. These actions include delay in gastric emptying time and enhancement of membrane lipid fluidity or direct draining of lymph into thoracic duct and further draining into the venous blood and inhibition of efflux transporters like p-glycoprotein (P-gp). It has been proven that it serves as an alternative approach to avoid the first-pass metabolism of drugs and improve bioavailability in peroral delivery.[23]

Even though several research works are being carried out to enhance the solubility and bioavailability of AM by formulating it as sublingual tablets, fast mouth dissolving film,[24] nanostructured lipid carriers for intranasal delivery,[25] nano-transfersomal formulations for transdermal delivery,[26] and *in situ* nasal gel,[27] still it is required to design the oral formulation having combined advantages such as sustained release and avoiding first-pass metabolism of AM using peroral route of delivery. Therefore, the aim of the present work was to improve the oral bioavailability of AM by formulating it as SLN.

Preparation of SLNs

In the present study, AM-loaded SLN were prepared by high-pressure homogenization method using Compritol 888 ATO as a lipid carrier. The method resulted in consistent production of smaller size nanoparticles (<260 nm) with narrow size distribution and good entrapment efficiency.

Experimental design and statistical analysis

The effect of formulation or process variables on the response parameters can be measured by constructing a mathematical model. Mathematical model helps in predicting values of response parameters at any selected values of formulation variables within the boundaries of the design. The levels of formulation variables which are intermediate between the selected levels may yield optimum formulation. Design Expert 10 software was used to generate a mathematical model for each response parameter and the subsequent statistical analysis.

The particle size and entrapment efficiency for the 9 batches (R_1 to R_9) showed a wide variation 80.6–258 nm and 70.73–80.45%, respectively [Table 2]. The data clearly indicate that the results of response variables strongly depend on the selected independent variables.

The coefficients of the polynomial equations generated using MLRA (Design-Expert 10) for particle size and % EE of AM-SLN dispersion were studied. Five coefficients (*a*–e) were calculated with k as the intercept.

$$Y = k + aX_1 + bX_2 + cX_1X_2 + dX_1^2 + eX_2^2 \ldots. \quad (2)$$

Polynomial equations obtained for response variables were as follows:

$$PS = +185.49 + 37.23X_1 - 45.57X_2 + 16.6X_1X_2 - 10.23X_1^2 + 9.77X_2^2 \quad (3)$$

$$EE = +74.00 + 2.33X_1 - 1.87X_2 + 1.91X_1X_2 + 3.33X_1^2 - 0.44X_2^2 \quad (4)$$

The equations can be used to obtain the estimates of the responses.

Factor X_1 (drug: lipid ratio) has a positive effect on both particle size and entrapment efficiency as indicated by the signs of

coefficient *a* (+37.23 and +2.33, respectively), whereas factor X_2 (number of homogenization cycles) shows a negative effect on particle size and entrapment efficiency as shown by the negative sign of coefficient *b* (−45.57 and −1.87).

Similarly, the effect of interaction term such as X_1X_2 on response variables can be seen from the signs and values of *c*. X_1^2 and X_2^2 terms are second-order terms and are useful to estimate non-linearity of response.

The criteria for the selection of suitable feasible region were primarily based on the highest possible values of % entrapment efficiency (>70%) and values of particle size which are <150 nm.

After studying the feasibility and intensive grids of formulation batches, three batches (A_1, A_2, and A_3) of SLN were prepared. The selected factor combinations from intensive grid with desired responses were selected and actually prepared. On the basis of particle size and entrapment efficiency obtained with optimized batches and numerical optimization, formulation A_2 is selected for further characterization and evaluation. Table 3 compares the predicted and experimental values. The low value of percentage error underlines the prognostic ability of selected design.

Table 2: Particle size and entrapment efficiency of AM-loaded SLNs (R1- R9) as per 3^2 factorial design

Formulation Code	Independent variables		Response variables	
	X_1	X_2	Particle size (nm)	% Entrapment efficiency
	Coded Level			
R_1	−1	−1	210	78.25
R_2	0	−1	230	75.94
R_3	+1	−1	258	78.77
R_4	−1	0	143	75.16
R_5	0	0	189	73.06
R_6	+1	0	204	80.45
R_7	−1	+1	80.6	70.73
R_8	0	+1	153	72.14
R_9	+1	+1	195	78.89

AM: Asenapine maleate, SLN: Solid lipid nanoparticles

From the results of experimental design, the utility of statistical design in screening of variables and manufacture of SLN was confirmed. Figure 1 shows the effect of lipid amount and homogenization cycles on particle size. An increase in the amount of lipid resulted in a corresponding increase in particle size. When lipid amount in external phase is increased, interfacial tension between lipid and aqueous phase increases, resulting in coalesce of globules, and thus increases in particle size. A significant decrease in the particle size and the range of particle distribution was observed on increasing the homogenization cycle. These results are in broad agreement with those reported by Yuan *et al*.[28]

The effect of lipid amount and homogenization cycles on the EE is illustrated in Figure 1. Gradual curvature for EE when viewed from lipid axis shows that an increase in the amount of lipid results in gradual increase in EE. An additional number of particles are provided by higher amount of lipid into which AM gets entrapped.

Evaluation of optimized batch of AM-loaded SLNs

Particle size, zeta potential, and entrapment efficiency

The particle size distribution of optimized batch A_2 is graphically represented in Figure 2. The polydispersity index of the same was found to be 0.34 ± 0.05, suggesting formation of a homogeneous dispersion. A low polydispersity index value demonstrates the narrow size distribution, which is the most significant parameter that decides the performance of nanoparticles in drug release and cellular uptake.[29]

Zeta potential is a key factor for evaluation of the stability of colloidal dispersion. Usually, particle aggregation is less likely to occur for charged particles with high zeta potential (>30 mV) due to electric repulsion.[30] The value of the zeta potential of AM-loaded SLN was found to be −41.4 mV which is sufficient to keep the particles stable [Figure 3].

Entrapment efficiency of optimized batch A_2 was found as 72.4%. High percentage EE can be attributed to the lipophilic nature of the drug, as it had a higher affinity for the lipid matrix.

Table 3: Comparison of experimental results with predicted responses

Batch Code	Composition* X_1/X_2 (Coded values)	Response	Predicted value	Experimental value	Percent error
A_1	−1/0	Particle size (nm)	138	144	−4.3
		Entrapment (%)	75.0	72.8	2.9
A_2	−1/0.5	Particle size (nm)	109	113	−3.7
		Entrapment (%)	73.0	72.4	0.8
A_3	−0.9/0.2	Particle size (nm)	132	136	−3.0
		Entrapment (%)	73.9	72.0	2.6

*Drug: lipid ratio/Number of homogenization cycles

Optimized formulation exhibited particles in nanometric size with high EE and low polydispersity index (PDI) value. Low PDI indicates that optimal conditions are suitable for the production of stable SLNs with narrow size distribution.

FE-SEM

SEM analysis of the optimized batch of AM-SLN was carried out to understand the morphology of SLN. Figure 4 shows the SEM image of spherical shaped and smooth surfaced particles of an optimized batch of AM-SLNs.

DSC

DSC thermograms [Figure 5] indicate the melting points and corresponding enthalpies of AM and AM-loaded SLNs. The enthalpy indicates absolute heat energy uptake and is given by area under transition peak. The sharp melting endotherm of AM was observed at 142.23°C with the corresponding enthalpy of 231.87 J/g. AM-loaded SLN showed endothermic peak at 77.65°C and enthalpy of 196.3 J/g. The melting endotherm of the drug was completely absent in the thermogram of AM-loaded SLN, which indicates that AM was completely solubilized inside the lipid matrix of the SLN and was not in a crystalline state in the formulation.

X-ray diffraction

From the X-ray diffraction data [Figure 6], it is clear that pure AM showed highly crystalline nature with principal peaks, whereas the SLN formulation showed deformed peak for AM, indicating its presence in amorphous or molecular dispersion state.

The diffraction patterns of the drug showed the remarkable difference from that of the SLN. The sharp peaks of drug and lipid were replaced by relatively broad peaks. It was clear that, from drug-loaded SLN, the less ordered crystals were majority and the amorphous state would contribute to the higher drug loading capacity as seen previously. There is a significant difference between the diffraction patterns of AM and AM-loaded SLN. It was confirmed that AM existed in amorphous state in the SLN because of the disappeared sharp peaks of AM in the diffraction pattern.

FTIR studies

From FTIR study, the characteristic peaks of drug such as of aromatic C-H stretch (3039 cm^{-1}), C-H stretch of methyl group (2925 cm^{-1}), C=O (1706 cm^{-1}), C-C stretch (1618, 1484 cm^{-1}), C-O stretching (1293 cm^{-1}), C=C stretch (1093 cm^{-1}), and aromatic C-Cl bends (655 and 587 cm^{-1}) disappeared and were replaced by the peak of Compritol 888 ATO. Remaining peaks also either shifted or replaced in

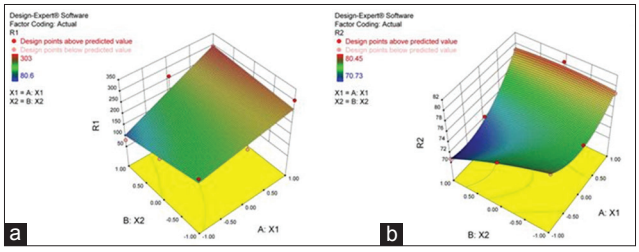

Figure 1: 3D response surface plot (a) particle size and (b) % entrapment efficiency

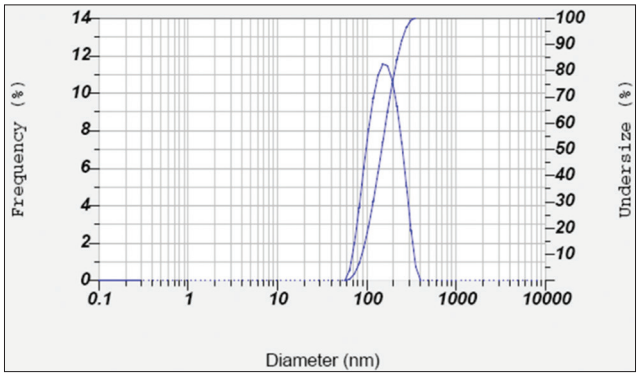

Figure 2: Particle size distribution curve of an optimized batch of drug loaded Solid lipid nanoparticles

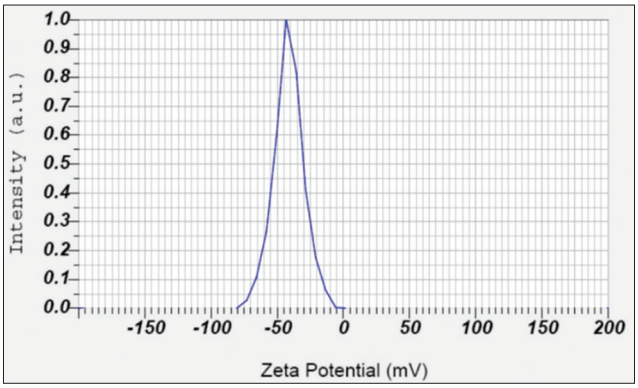

Figure 3: Zeta potential of an optimized batch of solid lipid nanoparticles

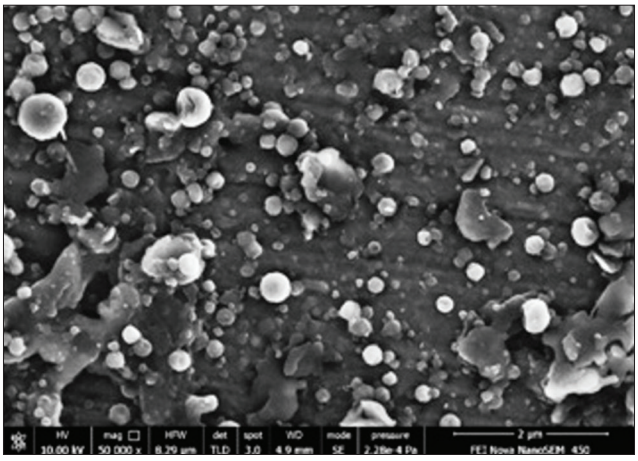

Figure 4: Scanning electron microscopy image of an optimized batch of solid lipid nanoparticles

the IR spectrum of formulation are shown in Figure 7. This established drug entrapment in a lipid matrix.

In vitro release of AM from SLNs

The results of release studies are represented graphically as cumulative % drug release versus time (h) as shown in Figure 8. In the present investigation, optimized formulation of AM-loaded SLN showed the controlled release of AM than dispersion of pure drug.

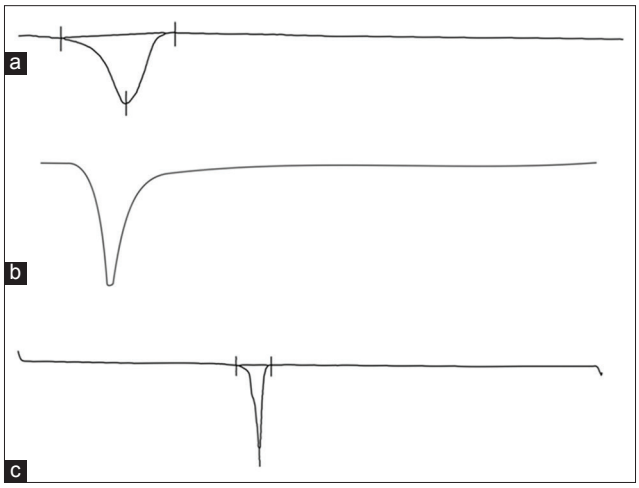

Figure 5: Differential scanning calorimetry thermogram of (a) Asenapine maleate solid lipid nanoparticles, (b) Compritol 888 ATO, and (c) asenapine maleate

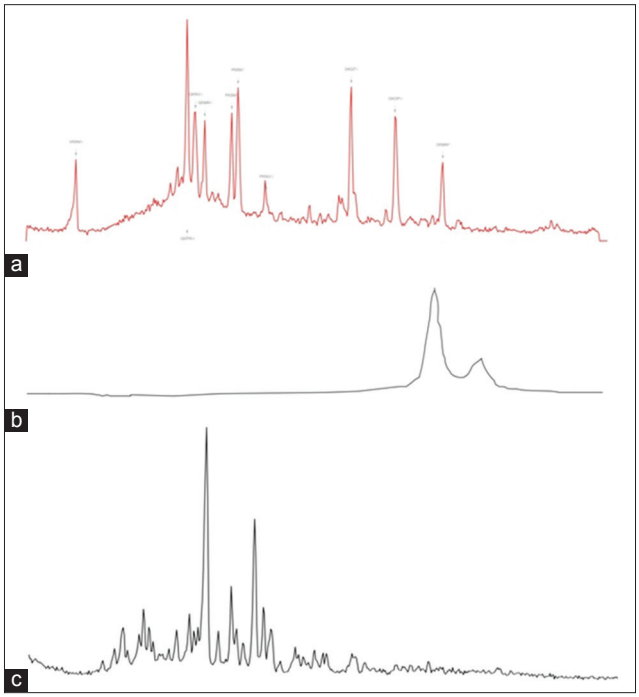

Figure 6: X-ray powder diffraction patterns of (a) asenapine maleate solid lipid nanoparticles, (b) Compritol 888 ATO, and (c) asenapine maleate

In SLNs manufactured by high-pressure homogenization technique, majority of incorporated drug remains in the core of lipid matrix. However, a portion of the drug remains bound at lipid surfactant interface. This results in biphasic drug release pattern from SLN. As evident from Figure 8, AM-loaded SLN presented initial burst release due to the surface presence of AM followed by more sustained release due to drug embedded in core of lipid matrix.

Pharmacokinetic studies

An *in vivo* pharmacokinetics study was evaluated on male Wistar rats [Figure 9], and statistical analysis of plasma drug concentration-time profiles was carried out using two-way ANOVA followed by Bonferroni post-test [Figure 10]. AM-loaded SLN showed the higher C_{max} in rat plasma by oral administration [Table 4]. It was found to be 142.41 ng/mL, while AM suspension showed the concentration of 77.02 ng/mL of drug in rat plasma. The AUC of AM-SLN was about 5-fold higher compared with the AM-suspension. AM-SLNs showed higher $t_{1/2}$ and MRT than AM-suspension, and this signifies slower drug elimination from the body. The increase in bioavailability is attributable to the uptake of the SLNs into the systemic circulation through the intestinal lymphatics. SLNs composed of triglycerides particularly resemble the chylomicrons and may alter the absorption behavior of drugs including avoidance of the first pass.[31] Intestinal lymphatic

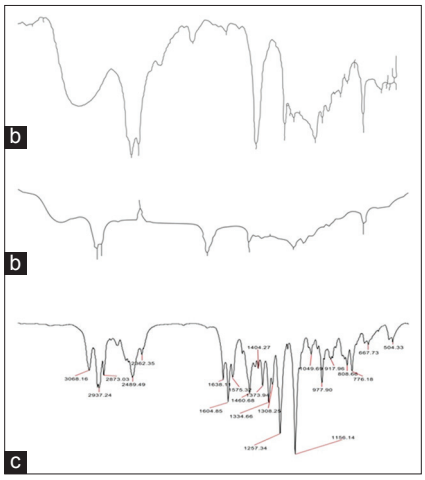

Figure 7: Fourier-transmission infrared spectra of (a) asenapine maleate solid lipid nanoparticles, (b) Compritol 888 ATO, and (c) asenapine maleate

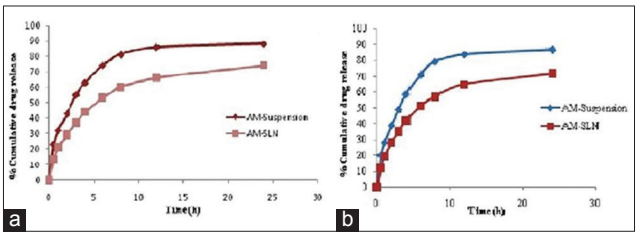

Figure 8: *In vitro* drug release of asenapine maleate in (a) 0.1 N HCl and (b) phosphate buffer pH 7.4

transport has the potential to enhance bioavailability through avoidance of first-pass metabolism in enterocytes as well as the liver and may influence drug activity and toxicity by altering drug clearance and distribution.[32]

In vivo brain distribution

It is evident from *in vivo* brain distribution study that the AM suspension-treated animal brain did not show any drug distribution in the brain [Table 5]. On the other hand, AM-SLNs showed a detectable AM concentration in the homogenate post-administration. This may be due to the poor oral bioavailability of AM as well as its extensive first-pass metabolism. Very negligible amounts of drug would have reached to brain tissues which are less than the lower limit of detection of the bioanalytical method used in this study.

Thus, the results of the present study proved that a large quantity of drug crossed the BBB after oral administration of AM-SLN and higher accumulation in the brain, thereby improving its bioavailability. Higher plasma concentration and brain distribution of oral AM administered as AM-SLN formulation could be a result of a number of factors.

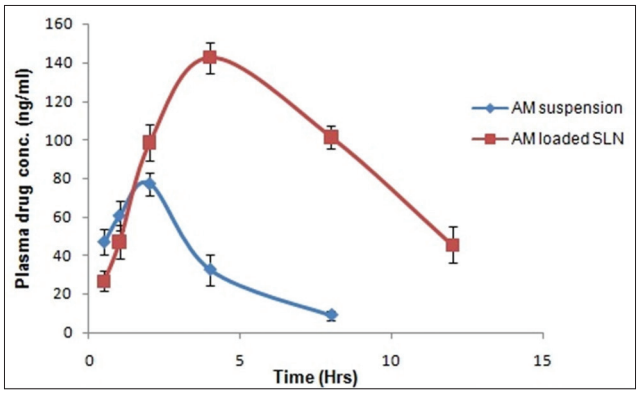

Figure 9: Plasma concentration-time profile of asenapine maleate (AM) suspension and AM-loaded solid lipid nanoparticles in rats

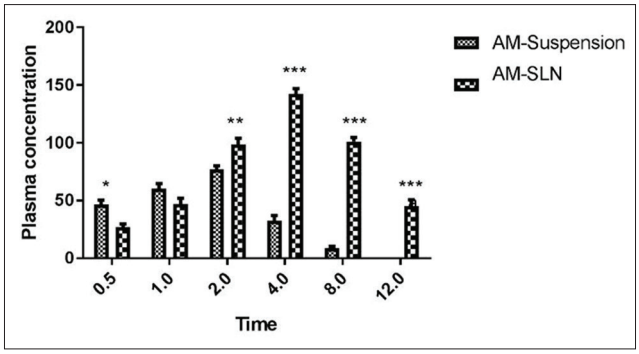

Figure 10: Statistical analysis of plasma drug concentration-time profiles. Two-way ANOVA followed by Bonferroni post-test. *$P < 0.05$, **$P < 0.01$, and ***$P < 0.001$ versus asenapine maleate suspension. Data are presented as mean ± standard deviation ($n = 6$)

Several mechanisms have been proposed for the transport of nanoparticles across the BBB. Many studies supported the mechanism of endocytosis.[33,34] Apolipoprotein B and/or E from the bloodstream get adsorbed by nanoparticles coated with polysorbate 80, where polysorbate 80 works mainly as an anchor. These nanoparticles overcoated with apolipoprotein would now mimic with lipoprotein particles and further taken up by the brain capillary endothelial cells through receptor-mediated endocytosis.[35] The prolongation of a drug's half-life in circulation was also proven to be important. The drug can be protected from metabolism and excretion when it is carried in SLNs. Besides endocytosis, nanoparticles can be transported by the paracellular pathway. The previous literature[36,37] indicated that both cationic and anionic nanoparticles can open tight junctions and thus allow passage of a drug across the BBB.

Overall, the results of our study suggest that AM-SLNs might be a promising nanocarrier system that can be used to improve the oral bioavailability and brain distribution of AM.

CONCLUSION

The present research work proposed a lipid nanoparticulate drug delivery system (SLNs) for oral delivery of AM. SLNs were prepared by the high-pressure homogenization technique and evaluated for particle size, zeta potential, entrapment efficiency, and *in vitro* release. All measurements were found to be in an acceptable range. Pharmacokinetics studies were performed on Wistar rats, in which the increase in the C_{max} and

Table 4: Results of pharmacokinetic analysis

Parameter	AM suspension	AM-loaded SLN
K_e	0.36±0.03	0.071±0.019
$T_{1/2}$(h)	1.96±0.18	10.18±2.47
C_{max} (ng/mL)	77.02±5.74	142.41±8.14
T_{max} (h)	2±0	4±0
AUC_{0-t} (ng/mL)	299.76±39.42	1561.81±36.34
$AUC_{0-\infty}$ (ng/mL)	325.44±47.94	1925.17±148.86
MRT (h)	2.73±0.16	15.31±3.21

AM: Asenapine maleate, SLN: Solid lipid nanoparticles, AUC: Area under the plasma concentration-time curve, MRT: Mean residence time

Table 5: Brain distribution studies

Time (h)	AM suspension (ng/mL)	AM-loaded SLN (ng/mL)
8	No drug detected in brain tissue	46.2±4.47
12		61.7±1.93

AM: Asenapine maleate, SLN: Solid lipid nanoparticles

AUC is indicative of lymphatic transport bypassing the hepatic first pass, thereby representing the superiority of AM-SLNs over AM-suspension. Further, brain distribution study showed higher drug permeation across the BBB and accumulation in the brain. It was concluded that AM-SLNs could be an effective drug delivery system for the treatment of psychiatric conditions like schizophrenia through oral route. However, clinical data are still needed to evaluate the risk: benefit ratio.

ACKNOWLEDGMENTS

We appreciate the generosity and cooperation of MSN Organics Pvt. Ltd., Telangana, India, for the gift sample of AM and Gattefosse, India, for the samples of excipients employed during the current studies.

REFERENCES

1. Moller HJ. Bipolar disorder and schizophrenia: Distinct illnesses or a continuum? J Clin Psychiatry 2003;64:23-7.
2. Tarazi FI, Shahid M. Asenapine maleate: A new drug for the treatment of schizophrenia and bipolar mania. Drugs Today 2009;45:865-76.
3. Bartlett JA, Maarschalk KV. Understanding the oral mucosal absorption and resulting clinical pharmacokinetics of asenapine. AAPS Pharm Sci Tech 2012;13:1110-5.
4. Stoner SC, Pace HA. Asenapine: A clinical review of a second-generation antipsychotic. Clin Ther 2012;34:1023-40.
5. Kapadia YD, Sodha, HP, Patel VP. Formulation development and evaluation of sublingual film of asenapine maleate. Pharm Sci Monitor 2013;4:190-209.
6. Van Der Sterren JE, Van Den Heuvel DJ, Inventor; Synthon BV, Assignee. Intranasal Administration of Asenapine and Pharmaceutical Compositions Therefor. United State Patent US No. 2008/0306133A1. 2008 Dec 11.
7. Faassen WA, Kemperman GJ, Van Laarhoven JH, Inventor; Organon NV, Assignee. Injectable Formulations Containing Asenapine and Method of Treatment using Same. World Patent WO No. 2010149727A3.2011 Apr 21.
8. Citrome L. Asenapine review, Part II: Clinical efficacy, safety and tolerability. Exp Opin Drug Safe 2014;13:803-30.
9. O'Driscoll CM. Lipid-based formulations for intestinal lymphatic delivery. Eur J Pharm Sci 2002;15:405-15.
10. Porter CJ, Charman WN. Intestinal lymphatic drug transport: An update. Adv Drug Deliv Rev 2001;50:61-80.
11. Charman WN, Porter CJ. Lipophilic prodrugs designed for intestinal lymphatic transport. Adv Drug Deliv Rev 1996;19:149-69.
12. Bargoni A, Cavalli R, Caputo O, Fundarò A, Gasco MR, Zara GP. Solid lipid nanoparticles in lymph and plasma after duodenal administration to rats. Pharm Res 1998;15:745-50.
13. Gambhire MS, Bhalekar M, Shrivastava B. Bioavailability assessment of simvastatin loaded solid lipid nanoparticles after oral administration. Asian J Pharm Sci 2011;6:251-8.
14. Yang S, Zhu J, Lu Y, Liang B, Yang C. Body distribution of camptothecin solid lipid nanoparticles after oral administration. Pharm Res 1999;16:751-7.
15. Mehnert W, Mader K. Solid lipid nanoparticles: Production, characterization and applications. Adv Drug Deliv Rev 2001;47:165-96.
16. Muchow M, Maincent P, Muller RH. Lipid nanoparticles with a solid matrix (SLN, NLC, LDC) for oral drug delivery. Drug Dev Ind Pharm 2008;34:1394-5.
17. Muller RH, Mader K, Gohla S. Solid lipid nanoparticles (SLN) for controlled drug – A review of the state of the art. Eur J Pharm Biopharm 2000;50:161-77.
18. Alam MI, Beg S, Samad A, Baboota S, Kohli K, Ali J, *et al.* Strategy for effective brain drug delivery. Eur J Pharm Sci 2014;40:385-3.
19. Kozlovskaya L, Abou-Kaoud M, Stepensky D. Quantitative analysis of drug delivery to the brain via nasal route. J Control Rel 2014;189:133-40.
20. Mistry A, Stolnik S, Illum L. Nanoparticles for direct nose-to-brain delivery of drugs. Int J Pharm 2009;379:146-57.
21. Dwivedi P, Khatik R, Khandelwal K, Taneja I, Raju KS, Wahajuddin M, *et al.* Pharmacokinetics study of arteether loaded solid lipid nanoparticles: An improved oral bioavailability in rats. Int J Pharm 2014;466:321-7.
22. Jensen LB, Magnussson E, Gunnarsson L, Vermehren C, Nielsen HM, Petersson K. Corticosteroid solubility and lipid polarity control release from solid lipid nanoparticles. Int J Pharm 2010;390:53-60.
23. Kushwaha AK, Vuddanda PR, Karunanidhi P, Singh SK, Singh S. Development and evaluation of solid lipid nanoparticles of raloxifene hydrochloride for enhanced bioavailability. BioMed Res Int 2013;Article ID: 584549:9.
24. Kokare CK, Tagalpallewar AA, Aragade PS, Bagul US, Bacchav RK, Nanjwade BK. Formulation, evaluation and optimization of asenapine maleate fast mouth dissolving film. J Pharm Sci Pharmacol 2015;2:194-207.
25. Singh SK, Dadhania P, Vuddanda PR, Jain A, Velaga S, Singh S. Intranasal delivery of asenapine loaded nanostructured lipid carriers: Formulation, characterization, pharmacokinetic and behavioral assessment. RSC Adv 2016;6:2032-45.
26. Shreya AB, Managuli RS, Menon J, Kondapalli L, Hegde AR, Avadhani K, *et al.* Nano-transfersomal formulations for transdermal delivery of AM: *In vitro* and *in vivo* performance evaluations. J Liposome Res 2016;26:221-32.
27. Kulkarni JA, Avachat AM. Pharmacodynamic and pharmacokinetic investigation of cyclodextrin mediated asenapine maleate *in situ* nasal gel for

improved bioavailability. Drug Develop Ind Pharm 2017;43:234-45.
28. Yuan Y, Gao Y, Zhao J, Mao L. Characterization and stability evaluation of b-carotene nanoemulsions prepared by high pressure homogenization under various emulsifying conditions. Food Res Int 2008;41:61-8.
29. Kharia AA, Singhai AK, Verma R. Formulation and evaluation of polymeric nanoparticles of an antiviral drug for gastro-retention. Int J Pharm Sci Nanotech 2012;4:1557-62.
30. Shrotriya SN, Ranpise NS, Vidhate BV. Skin targeting of resveratrol utilizing solid lipid nanoparticle-engrossed gel for chemically induced irritant contact dermatitis. Drug Deliv Transl Res 2017;7:37-52.
31. Singh I, Swami R, Khan W, Sistla R. Lymphatic system: A prospective area for advanced targeting of particulate drug carriers. Expert Opin Drug Deliv 2014;11:211-29.
32. Hea-Young C, Yong-Bok L. Nano-sized drug delivery systems for lymphatic delivery. J Nanosci Nanotech 2014;14:868-80.
33. Wilson B, Samanta MK, Santhi K, Kumar KP, Paramakrishnan N, Suresh B. Poly(n-butylcyanoacrylate) nanoparticles coated with polysorbate 80 for the targeted delivery of rivastigmine into the brain to treat Alzheimer's disease. Brain Res 2008;1200:159-68.
34. Kreuter J. Nanoparticulate systems for brain delivery of drugs. Adv Drug Deliv Rev 2001;47:65-81.
35. Kreuter J, Shamenkov D, Petrov V, Ramge P, Cychutek K, Koch-Brandt C, *et al*. Apolipoprotein-mediated transport of nanoparticle-bound drugs across the blood brain barrier. J Drug Target 2002;10:317-25.
36. Lockman PR, Koziara JM, Mumper RJ, Allen DD. Nanoparticle surface charges alter blood-brain barrier integrity and permeability. J Drug Target 2004;12:635-41.
37. Tosi G, Costantino L, Ruozi B, Forni F, Vandelli MA. Polymeric nanoparticles for the drug delivery to the central nervous system. Expert Opin Drug Deliv 2008;5:155-74.

Source of Support: Nil. **Conflict of Interest:** None declared.